

# D11.4

## MODEM CONSTELLATION IDENTIFICATION: A PERFORMANCE COMPARISON OF TWO METHODS

Sally L. Wood

Michael G. Larimore

John R. Treichler

EECS Department  
Santa Clara University  
Santa Clara, CA, 95053  
(408) 554-4058

Applied Signal Technology  
160 Sobrante Way  
Sunnyvale, CA, 94086  
(408) 749-1888

### ABSTRACT

Interest has grown in the last few years in multi-drop networks for voice channel modems where each modem in sequence broadcasts to all others on the network. Several modem manufacturers have developed procedures for operating in this fashion, including provisions for initializing all of the modems "listening" to the designated transmitter. This initialization is made more complicated by the advent of trellis-coded modems (TCMs) which can operate with any of a variety of signal constellations. It is compounded further if the user desires to enter and leave the network at any time – an operational mode that requires the initialization process to be conducted without the active cooperation of the transmitter. Previous work by the authors has examined a Radon transform based method for identification of the signal constellation in use [1,2]. Others have recently suggested the use of alternative methods which use only the magnitude or "radius" of the received signal to identify the constellation size. This paper begins a comparison of these methods with a focus on detection performance as a function of the constellation's signal-to-noise ratio. It is shown that the Radon transform method performs at lower SNRs than a candidate radius-only method, albeit at the cost of having to estimate the carrier frequency. An extension of the Radon transform method which allows some carrier frequency uncertainty is also mentioned.<sup>1</sup>

### Introduction

Interest has grown in the last few years in multi-drop networks for voice channel modems where one modem at a time broadcasts to all others on the network. Several modem manufacturers have developed procedures for operating in this fashion, including provisions for initializing all of the modems "listening" to the designated transmitter. Careful initiation procedures are needed to quickly attain the equalization, baud-rate tracking, and carrier tracking needed for proper demodulator operation. Traditionally, these procedures require the active cooperation of the transmitter in the form of transmitted training sequences. A significant problem in the use of multi-drop networks is that the introduction of a new receiver implies a new training effort, with associated loss of data throughput. The loss of data throughput is related to the number of modems on the network and the average number of times each one leaves and then reenters the network. It is thus highly desirable to develop methods of "passively" obtaining the required set-up information at the receiver. The problem is further exaggerated by new classes of trellis-coded modems (TCMs) which are not only difficult to equalize and carrier track, but can operate with any of a variety of signal constellations depending on prevailing circuit conditions. When using these modems, a new receiver will be uncertain as to the constellation currently in use, as well as the carrier frequency and phase and the proper equalization filter.

<sup>1</sup>This work was supported by NSF grant #86-98035 and by Applied Signal Technology, Sunnyvale California.

Considerable work has been done in the area of blind equalization, that is, equalizing the propagation channel's effects on a signal without clear knowledge of the transmitted carrier frequency and constellation. Methods have also been developed for acquisition of the signal's carrier frequency and phase. This paper focuses on the problem exaggerated by the use of TCMs, identification of the signal constellation in use. For simple constellations, such as the square used in QPSK, simple trial and error is adequate. For more complicated ones, however, such as the 256-point constellations used in 16.8 kb/s TCMs, identification can be difficult, particularly in the presence of additive noise or incomplete equalization. An earlier ICASSP paper [1] proposed and analyzed a constellation identification method based on the Radon transform. Another paper [2] examined certain performance properties of the method when used in the presence of additive noise and unequalized dispersion. This method was shown to be reliable for square, hexagonal, and cross constellations ranging in size from 4 to 256 points, even when the signal is not fully equalized and carrier-locked. The method works for signal-to-noise ratios poorer than those supporting bit-error rates of 0.1, meaning that identification can be accomplished for any practically demodulable signal.

The Radon transform method uses blindly-equalized complex waveform samples, and requires that the signal's carrier frequency be known fairly accurately. Other methods, based on histogramming the blindly-equalized signal's magnitude, have been suggested by a number of workers. The principal advantage of this approach is that the carrier frequency need not be known at all. To date no performance analysis has been reported for any of the suggested magnitude-histogram methods and therefore no meaningful comparisons have been done between the two. This paper begins to fill that gap, comparing the performance of two schemes, one a technique based on the Radon transform and another a "radius-only" method. The two methods are each described and then are compared as a function of such variables as the signal-to-noise ratio, the number of samples needed, the constellation size, and the carrier phase uncertainty. The final section summarizes the work presented in the paper and points out areas in which more work is needed in order to reach conclusive results.

### Two Dimensional Constellation Model

The ideal square array can be described mathematically as the convolution of two one-dimensional finite extent arrays of regularly spaced impulses. Let  $L(x, y)$  represent an ideal  $M \times M$  array written as

$$\begin{aligned} L(x, y) &= \sum_{i=0}^{M-1} \delta(x - x_i) * \sum_{j=0}^{M-1} \delta(y - y_j) \\ &= \sum_{i=0}^{M-1} \sum_{j=0}^{M-1} \delta(x - x_i, y - y_j) \end{aligned} \quad (1)$$

where

$$\begin{aligned} x_i &= (2i - (M-1))\Delta_x/2 & \text{for } 0 \leq i < M \\ y_j &= (2j - (M-1))\Delta_y/2 & \text{for } 0 \leq j < M \end{aligned} \quad (2)$$

A complete square array is thus separable in the  $x$  and  $y$  variables. Cross constellations can be generated from the square arrays by windowing, and hexagonal arrays are the sum of two offset rectangular arrays with appropriate windowing. Each observed signal point  $s_{ij}$  will occur in some neighborhood of the ideal point  $(x_i, y_j)$  with a probability density function depending on the noise statistics. Identification of the constellation type can be made based on characteristic point separations and rotational symmetry.

Let the probability of observing a point offset from its ideal position by  $x$  and  $y$  be given by  $P_c(x, y)$ . Let  $H_N(x, y)$  represent the two dimensional histogram of  $N$  observations. As the number of observations grows large, an appropriately scaled histogram  $H_N(x, y)$  of observed points will approach the limit

$$\lim_{N \rightarrow \infty} H_N(x, y) = L(x, y) * P_c(x, y) \quad (3)$$

and  $\mathcal{H}_N(x, y)$ , the two dimensional Fourier transform of  $H_N(x, y)$  will approach the limit given by

$$\lim_{N \rightarrow \infty} \mathcal{H}_N(u, v) = \mathcal{L}(u, v) \cdot \mathcal{P}(u, v) \quad (4)$$

where  $\mathcal{L}(u, v)$  is the transform of the finite lattice pattern. Thus  $\mathcal{L}(u, v)$  is a lattice with reciprocal spacing convolved with sinc functions determined by the total extent of  $L(x, y)$  and is represented by

$$\mathcal{L}(u, v) = \frac{\sin \pi M \Delta_x u}{\sin \pi \Delta_x u} \frac{\sin \pi M \Delta_y v}{\sin \pi \Delta_y v} \quad (5)$$

Peaks in  $\mathcal{L}(u, v)$  will occur at multiples of  $u_0 = 1/\Delta_x$  and  $v_0 = 1/\Delta_y$ . Peaks at these positions in  $\mathcal{H}_N(u, v)$  will be attenuated by the shape of the probability density function  $\mathcal{P}(u, v)$ . For low noise environments  $\mathcal{P}(u, v)$  will have significant amplitude well beyond  $u_0$  and  $v_0$  so several peaks in the transform domain will be detected at multiples of  $u_0$  and  $v_0$ . As the average amplitude of the noise increases, the probability density function  $P_c(x, y)$  will broaden, which in turn will increase the attenuation of the peaks at multiples of  $u_0$  and  $v_0$ . As the noise amplitude continues to increase, eventually the increased attenuation of the peak at  $u_0$  causes it to be undetectable, corresponding to an almost uniform distribution of points. When this condition occurs, constellation identification can not be made reliably. When a finite number of observations are used,  $H_N(x, y)$  can be considered to be its expected value with added noise that decreases as  $N$  increases. To guarantee detectability in this case, the attenuation of the peak at  $u = u_0$  by  $\mathcal{P}(u, v)$  must be less than the noise level due to a small number of observations. Thus, both the number of observations and the ratio of the point spacing to the standard deviation of the added noise will affect the identifiability of a constellation. In Figure 1 a 64-point noise-free square lattice is shown next to 1024 samples from that constellation with added noise corresponding to a 10% symbol error rate. In the transform domain, the peak at  $u_0$  is easily detected for this noisy data.

The Radon transform offers a computationally attractive alternative to the two dimensional Fourier transform for constellation identification. The Radon transform converts a function of  $x$  and  $y$  to a function of  $\rho$  and  $\theta$  by taking line integrals through the original function along all possible lines where a line is specified by orientation,  $\theta$ , and distance,  $\rho$ , from the origin. The mathematical definition is given by



Figure 1: Ideal and noisy 64 QAM constellation

$$\begin{aligned} F(\rho, \theta) &= \int F(x, y) dl_{\rho, \theta} \\ &= \iint F(x, y) \delta(\rho - x \cos \theta - y \sin \theta) dx dy \end{aligned} \quad (6)$$

Let a slice of constant  $\theta$  through the Radon transform be defined as  $f(\rho)_{\theta=\theta_0}$ . It is well known and easily demonstrated that a one dimensional Fourier transform of  $f(\rho)_{\theta=\theta_0}$  with respect to variable  $\rho$  will yield a "slice" of the two dimensional Fourier transform of  $F(x, y)$  taken through the origin of transform space at angle  $\theta_0$  [3]. Thus, a one dimensional transform of the projection taken at the angle corresponding to the square constellation orientation will show a peak at  $\rho = u_0 = v_0$ . The width or radius of the peak is determined by the finite extent of the constellation and can be detected within a specific range of the correct orientation. Although other peaks may be detected at other orientations, they will always be of less amplitude than the main peak at  $\rho_0$ .

For a lattice defined by Equation 1 the Radon transform is given by

$$L(\rho, \theta) = \sum_{i=0}^{M-1} \delta(\rho - x_i \cos \theta) * \sum_{j=0}^{M-1} \delta(\rho - y_j \sin \theta) \quad (7)$$

A projection taken at  $\theta = \theta_0$ ,  $l(\rho)_{\theta=\theta_0}$  can be obtained from Equation 7 by fixing the value of  $\theta$ . This function of one variable,  $\rho$ , is a convolution of  $M$  impulses spaced by  $\Delta_x \cos \theta_0$  with another  $M$  impulses spaced by  $\Delta_y \sin \theta_0$ . When  $\theta_0$  is aligned with the lattice pattern  $M$  impulses will coincide at each of  $M$  positions spaced by  $\Delta_x$  or  $\Delta_y$ . If  $\theta_0$  is rotated by  $\pi/4$  there is reinforcement with a triangular envelope and spacing of  $\Delta\sqrt{2}/2$ . The Radon transform of  $P_c(x, y)$  at each angle  $\theta$  will be convolved with the impulse sequence from Equation 7.

The main advantages of using the Radon transform followed by one dimensional Fourier transforms are computational. The angular resolution can be chosen independently from the spatial frequency resolution, rotational symmetry can be used, and a square histogram bin with orientation preference is not needed. Four cases can be considered for identification of the constellation spacing and rotational symmetry. In the first case the carrier is assumed to be locked and the phase, or constellation orientation, is known. In the second case, the phase is assumed unknown, but constant. In the third case some error in the carrier frequency may be present causing the constellation to rotate at a constant rate. In the fourth case, the carrier is assumed fixed, but the phase can rock within angular limits of uncertainty.

### One Dimensional Modulus Method

An alternative constellation identification method based on a one dimensional modulus distribution offers certain practical advantages since it can be used in the absence of local carrier synchronization. Given only proper symbol

rate synchronization, the complex constellation “spins” at a rate determined by the tuning error of the local oscillator. In the presence of spin, a noisy constellation becomes a set of concentric rings; the pattern of rings is unique to each constellation structure and can be used as a feature for identification. However, exploitation of modulus structure effectively collapses information about the symbol distribution in the complex plane to a single dimension, and as a result, at least under certain conditions, suffers degradation in detection performance.

Consider the  $8 \times 8$  64-QAM constellation shown in Figure 1, normalized to unity power by the receiver’s gain scaling. For a very low noise level the received symbols form small circular Gaussian clusters about their noise-free values. However, in the absence of carrier synchronization the constellation appears as shown in Figure 2a where the noise level corresponds to a symbol error rate of  $10^{-6}$ ; note that there are nine distinct rings, or modulus values, that form a “fingerprint” for this 64-point structure. The rings are non-uniformly spaced (by factors of 3.5 to 1) and have different

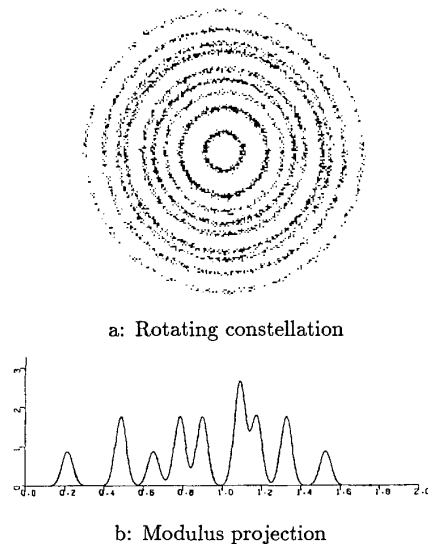


Figure 2: Modulus projection of noisy rotating constellation

intensities (by factors of 3 to 1); intensity variations equate to the probability of occurrence. Mathematically, we can represent such a ring pattern in terms of a one-dimensional modulus density function, shown in Figure 2b. Note for this case that there are nine modulus peaks with small Gaussian variations due to the additive noise.

Obviously, the distinct nature of the modulus distribution “fingerprint” is degraded with increasing noise level. As the variance about each peak increases, the depressions distinguishing them disappear, smearing together those with smallest separation. Consequently, a robust detection algorithm must not rely on the full set of density features (peaks and valleys), but rather on those visible at the desired noise level. Thus, we may use the distance of feature separation as a means of quantifying the loss incurred by reducing a constellation to its modulus density. That is, suppose symbols are separated by  $\Delta$  in the complex plane; signal quality (i.e. error rate) is typically related to the quantity  $\Delta/\sigma$ , where  $\sigma$  is the standard deviation of the Gaussian noise in one dimension.

By necessity the separation of modulus levels can be

no more than  $\Delta$ , and in fact, may be significantly less. For example, in the square 64-QAM case, modulus separation ranges from  $0.27\Delta$  for two peaks near the high end, to  $0.87\Delta$  for the two lowest peaks. Thus, in a sense, detection performance based on recognition of the two most distinct peaks will be degraded by about 1.2 dB from that achievable when using the entire two-dimensional distribution; requiring several such peaks to reduce false alarms will degrade noise immunity by several more dB.

## Performance Results

Simulated input sequences were created for 64 QAM, 256 QAM and a 64 point hexagonal constellation taken from [4]. Gaussian noise was added with variance controlled to generate symbol error rates of 1% and 10%. Both the Radon transform and the modulus method were used to identify the constellations as a function of noise level and number of samples. Performance was measured by the number of samples required to achieve reliable identification. For both methods thresholds were set so that the false alarm rate was 10% or lower. By altering thresholds, a ROC could be derived for each method.

**One Dimensional Modulus Method Performance:** The authors are aware of at least several distinct approaches for identification through modulus exploitation, resulting in algorithms tuned for specific applications, e.g. identification rate, signal quality, simplicity, etc. For purposes of demonstration, we present a simple feature-based selection method. The intent of this paper is to demonstrate the workings of such a method in a general sense, and as a result, no attempt was made to optimize the specific detection rules. Modulus information is recorded into a histogram of 256 bins, spanning 0 to 2. Then, bin groupings are combined into features unique to a specific constellation. The algorithm demonstrated here specifically addresses the square 64-QAM structure. The histogram is reduced to 10 features, locations of most pronounced clusters and depressions that distinguish the density from other candidates. The set of rules relating the features is tested at the end of the observation interval, and a detection decision made.

Figure 3 summarizes the performance of the algorithm as a function of observation interval for two levels of signal quality. For 22 dB SNR, the signal’s inherent error rate is about 1%, and reliable detection (90%) is achieved after about 350 symbols are recorded. In the second case, the signal’s quality is reduced to about the 10% error level (19 dB SNR) and reliable detection is achieved after more than 1000 symbols; this quality is often cited as a bound at which decision-aided equalization/tracking algorithms are effective. Such algorithms rely on knowledge of the constellation structure to achieve final carrier synchronization and channel equalization. The loss of 3 dB increases the detection time by about a factor of three. For completeness, false alarm performance is shown as well. For the given selection rules, a record of nearly circular uniform noise is mistaken for 64-QAM well under 10% of the time; for longer observation intervals the false alarm rate is essentially zero.

**Radon Transform Method Performance:** Resolution requirements were selected to achieve success for the case in which the carrier frequency is locked but the phase is unknown and slowly time-varying. Samples with normalized power were accumulated in 16 angular bins over  $90^\circ$  to detect 8 fold symmetry and in another 16 angular bins over  $60^\circ$  to detect 12 fold symmetry. In each angular bin projection values were quantized and accumulated in 256 bins spanning the range from 0 to 2. Since even symmetry was guaranteed over the range -2 to +2, the spatial frequency resolution was 0.25 cycle. Using characteristic point separations for the three constellations of interest, the peaks in the frequency domain for the 64 and 256 QAM signals should occur at 3.24 cycles (bin 12.96) and 6.41 cycles (bin 25.62) respectively for the projections enhancing 8 fold symmetry.

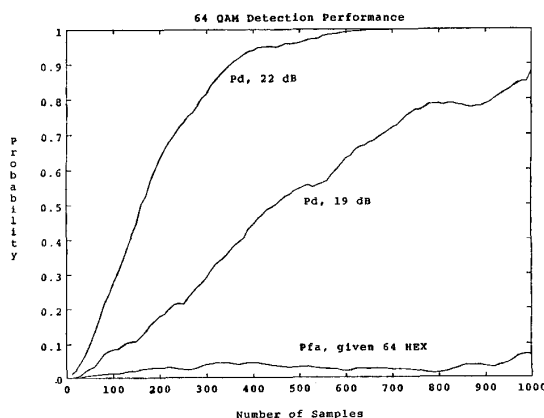


Figure 3: Performance of one dimensional modulus method

The hexagonal constellation will have a peak at bin 13.71 (3.43 cycles) in the projections enhancing 12 fold symmetry. Performance would not be degraded by using 128 points instead of 256, since the maximum frequency would still be more than four times larger than the highest frequency of interest. However 256 point resolution was chosen to be consistent with the magnitude method.

The magnitude of the characteristic frequency of a constellation is compared to the average amplitude of all frequencies above 2 cycles, and this ratio is used to detect the spacing, symmetry, and orientation of a constellation. The frequency with the largest magnitude in any projections is determined and then, after normalization by the average magnitude, is compared to a threshold. A ratio threshold of four is conservative in that false alarms are virtually nonexistent and detection can be made in a relatively small number of samples. For these tests, the frequency amplitude was taken from the nearest bin frequency rather than interpolating for fractional bin values. Explicit magnitude computations are not needed because of symmetry conditions. Improved amplitude estimation could be made from an interpolated value or by using a matched filter for a few specific constellations.

For the 64-QAM constellation with a 10% symbol error rate,  $\sigma/\Delta$  has a value of 0.26. The ratio of the peak to average amplitude of the characteristic frequency consistently begins to diverge from the other two frequencies after about 32 observations. An average of normalized characteristic frequency amplitudes for 50 test sequences of 256 points is shown in Figure 4a where the octagon, square, and diamond indicate the 64 point, 256 point, and hexagonal constellations respectively. The ratios for the 256 and hexagonal frequencies averaged 1.0 and rarely exceeded 3.0 in any test. The ratio at the characteristic frequency for the 64-QAM constellation averages approximately 5 after 64 observations and 10 after 256 observations. It continues to increase roughly with the square root of the number of observations corresponding to the decrease in variance of the average amplitude. With a decision threshold of 3.5, the probability of detection, shown in Figure 4b, exceeds 90% after 80 samples with no false alarms. If the phase is uniformly distributed over  $11.25^\circ$ , 128 samples are needed to achieve 90% detection. Peak to average and detection curves for the 256 point constellation are almost identical to the 64 point constellation for a 10% SER since the value of  $\sigma/\Delta$  is the same. For the hexagonal constellation a 10% SER corresponds to  $\sigma/\Delta = 0.29$  when  $\Delta$  is interpreted as the effective separation when rows are aligned. For that case, 1024 points are needed for reliable identification. For the 64-QAM constellation with a 1% SER and  $\sigma/\Delta = 0.18$ , reliable identification was made with 32 samples.

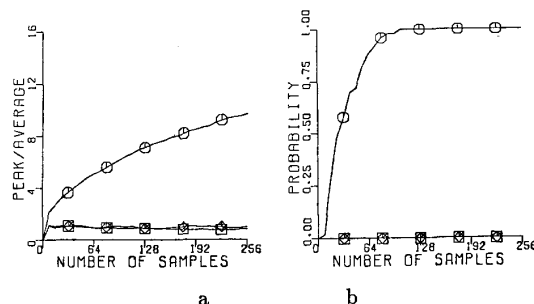


Figure 4: Radon transform method for 10% SER: (a) Peak to average ratio and (b) Probability of identification

## CONCLUSIONS

This paper describes two algorithms for determining the signal constellation in use on a QAM modulator, one based on Radon transform ideas and the other based on histogramming received signal radius information. The detection performance of the two specific algorithms were compared as a function of the signal-to-disturbance power ratio and the number of samples available. Generally speaking it is shown that when the carrier frequency is known with reasonable accuracy then the Radon transform method performs much better than the specific radius- or magnitude-only method tested here, in the sense that for the same signal-to-disturbance ratio the former can reliably determine the constellation size and orientation with about one-tenth of the data samples required by the latter. It should be noted, however, that neither or the two algorithms has been optimized nor have the comparisons taken into account other issues such as the details of particular applications, the relative computational requirements, and the added complexity needed by the Radon transform method to deal with uncertainties in the carrier frequency. These issues needed to be examined in more detail before the results can be stated conclusively.

## REFERENCES

- [1] S.L. Wood, et al., "Constellation Identification Using the Radon Transform", *Proc. 1988 International Conference on Acoustics, Speech, and Signal Processing*, New York, NY, April, 1988.
- [2] S.L. Wood and J.R. Treichler, "Performance of the Radon Transform Method for Constellation Identification", *Proc. 1988 Asilomar Conference on Circuits and Systems*, Asilomar, CA, 31 Oct 88.
- [3] R.N. Bracewell, "Strip Integration in Radio Astronomy", *Australian J. of Physics*, Vol. 9, No. 2, pp198-217, 1956.
- [4] G.D. Forney, et al, "Efficient Modulation for Bandlimited Channels", *IEEE Journal on Selected Areas in Communication*, vol SAC-2, Sept., 1984, pp632-641.